Deep-Sea Research, Vol. 38, Suppl. 1, pp. S63–S82, 1991.
Printed in Great Britain.

0198–0149/91 $3.00 + 0.00

Transpacific sections at 47°N and 152°W: distribution of properties

LYNNE D. TALLEY,* TERRENCE M. JOYCE† and ROLAND A. DESZOEKE‡

(*Received* 13 *November* 1989; *in revised form* 16 *August* 1990; *accepted* 31 *August* 1990)

Abstract—Three CTD/hydrographic sections with closely-spaced stations were occupied between May 1984 and May 1987, primarily in the subpolar North Pacific. Vertical sections of CTD quantities, oxygen and nutrients are presented. Upper water properties suggest that the Subarctic Front is located south of the subtropical/subpolar gyre boundary at 152°W, that there is leakage of North Pacific Intermediate Water from the subtropical to the subpolar gyre in the eastern Pacific, and verify the poleward shift of the subtropical gyre center with depth. At intermediate depths (1000–2000 m), a separation between the western and eastern parts of the subpolar gyre is found at 180° along 47°N. Abyssal waters are oldest in the northeast, with primary sources indicated at the western boundary and north of the Hawaiian Ridge. Properties and geostrophic velocity from detailed crossings of the boundary trenches suggest that flow in the bottom of the Kuril–Kamchatka Trench at the western boundary at 42°N and 47°N is northward. Very narrow boundary layers at intermediate depths are revealed in silica, as well as in the dynamical properties, at both the western and northern boundaries, and probably reflect southward and westward flow.

1. INTRODUCTION

IN the past five years, several new hydrographic data sets have been collected in the North Pacific using a sampling philosophy that differs substantially from the past. These include a zonal section along a nominal latitude of 47°N, data collected on a separate cruise which completes the 47°N section off Kamchatka, and a meridional section along a nominal longitude of 152°W. A transpacific section at 24°N is described elsewhere (ROEMMICH *et al.*, 1991), and a fourth along 10°N has been completed recently. In addition, closely-spaced sections across the Aleutian Trench at 165°W and 175°E (WARREN and OWENS, 1985, 1988) fit well with this modern data set.

Other than on these cruises, a substantial amount of fairly high quality data including oxygen and nutrient observations has been collected in the North Pacific. Station separation has been wide, but coverage has been sufficient to allow large-scale patterns of tracers and dynamic height to be mapped at all depths. Prior to the new data collections, boundary regions and steep topography had not been properly sampled.

The new observations take advantage of the old in that new, broad-scale sampling is not really necessary, even though the accuracy of the prior data was not ideal. Even though the

*Scripps Institution of Oceanography, University of California, San Diego, La Jolla, CA 92093, U.S.A.
†Woods Hole Oceanographic Institution, Woods Hole, MA 02543, U.S.A.
‡College of Oceanography, Oregon State University, Corvallis, OR 97333, U.S.A.

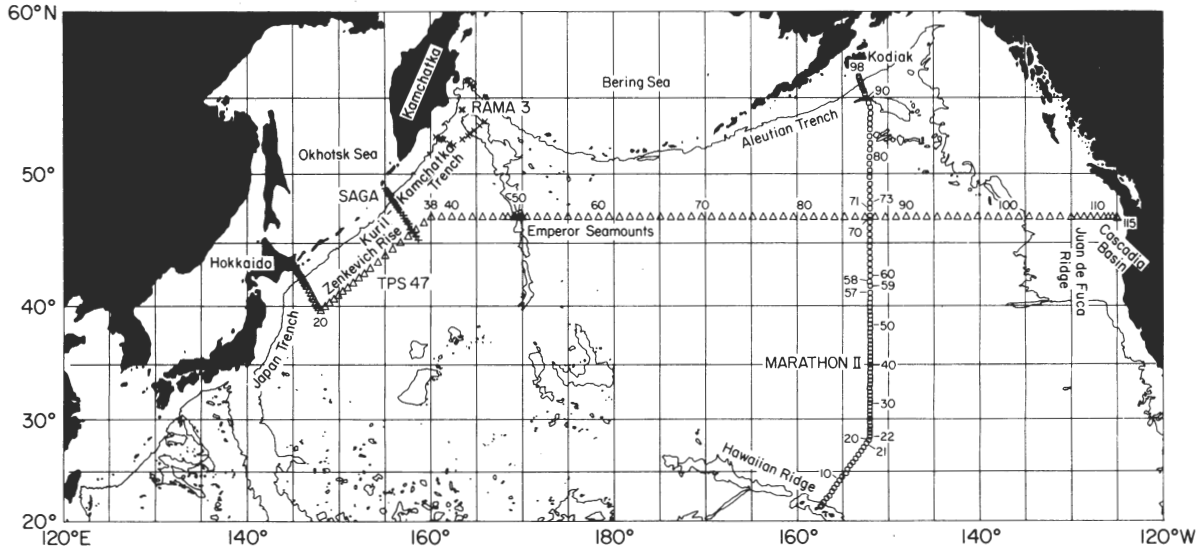

Fig. 1. TPS47 stations occupied by R.V. *T. Thompson* to the bottom between 4 August and 7 September, 1985 (triangles), SAGA II stations in the northwest Pacific, occupied by the *Akademik Korolev* between 11 May and 18 May, 1987 (+s), and MARATHON II stations occupied by R.V. *T. Washington* between 4 May and 4 June, 1984 (circles).

primary reason for the close station spacing typical of the new data sets was to obtain adequate estimates of geostrophic velocities and transports across the entire section lengths, the spacing and careful boundary sampling permit us to map smaller scale features that are an important part of the long-term, large-scale circulation. ROEMMICH and MCCALLISTER (1989) have used the 47°N and 152°W data described in this paper as part of their North Pacific inverse model to estimate transports from one region to another. We also are preparing a full description of the velocities and transports from 47°N, using both the observed density and acoustic Doppler current profiler (ADCP) data.

Section 2 of this paper contains descriptions of the vertical sections of water properties displayed on the color plates accompanying this issue. Section 3 summarizes some of the features which are evident in several of the sections, using isopycnal distributions and simple velocity calculations.

2. DATA COLLECTION

A. 47°N: TPS47 and SAGA II

In August 1985, a set of 115 relatively closely-spaced CTD/rosette stations was occupied by R.V. *T. Thompson* along a nominally-zonal line in the subpolar North Pacific. The cruise is henceforth referred to as TPS47. The stations (Fig. 1) were located along 47°N except in the west, where the cruise started with a section southeastward from Hokkaido and then jogged north to 47°N. Station spacing was nominally 80–85 km, with spacing increasing from 30 to 70 km between Stas 12 and 30 and decreasing from 54 to 34 km from Sta. 106 to 114. Over steep topography we based our station positions roughly on 750 m isobath separations; the resulting transport calculations are still somewhat sensitive to the method of isopycnal slope extrapolation, although ROEMMICH *et al.* (1991) show through a comparison of fully sampled and subsampled versions of TPS24 data that

this choice of station separation is fairly good. All stations extended to 6000 m or the bottom, whichever was shallower, with one station to 6240 m in the Kuril–Kamchatka Trench.

The second set of stations was collected in May 1987, during the SAGA II expedition of the *Akademik Korolev*, henceforth referred to as SAGA. All but one of the 23 northwest Pacific stations (Fig. 1) extended to 6000 m or the ocean bottom, whichever was shallower. An additional 37 shallow stations collected between 40°N and 29°S at 2.5° spacing along 160°E are not discussed here. The northwest Pacific stations were collected specifically to complete the TPS47 data set, closing off the zonal section at the northern Kuril Islands.

B. 152°*W*: *M2*

Ninety-seven stations collected between 4 May and 4 June 1984, along a nominal longitude of 152°W from Oahu to Kodiak Island, are also included in this discussion. Asterisks on the color plates indicate irregular station numbering. This section was made during the second leg of the MARATHON expedition of R.V. *T. Washington* and is henceforth referred to as M2. Station spacing was nominally 45 km between Oahu and 28°N and between 41°N and Kodiak; in the broad frontal region from 28° to 41°N, spacing was reduced to 33 km. At the northern and southern boundaries, it was reduced based on topography, in the same way as described for TPS47. Because of time limitations, station depths between 22°30′N and 52°32′N alternated between 1500 m and full ocean depth.

C. Data

Data from TPS47, SAGA and M2 were collected and processed by the Oceanographic Data Facility (ODF) at Scripps Institution of Oceanography. A full report of the M2 data is found in Martin *et al.* (1987), and reports of the TPS47 and SAGA data are in Talley *et al.* (1988a,b). Stations on all cruises consisted of CTD/rosette casts to within 10 m of the bottom except as indicated above. A Neil Brown Mark III CTD was used for all cruises. A 24-bottle rosette was used on M2 and SAGA; a 36-bottle rosette was used on TPS47. Salinity, oxygen, silica, nitrate, nitrite and phosphate were measured at nominally every bottle. The vertical sections distributed with this issue show CTD potential temperature and salinity, and discrete oxygen and nutrients; the latter sections show all the depths at which successful measurements were made.

CTD temperature accuracy depends on the laboratory calibration standard and the drift of the platinum resistance thermometer during the cruise. Laboratory calibration accuracy in 1984–1985 was 0.001°C and in 1987 was 0.0005°C (J. Swift, personal communication). Pre- to post-cruise temperature drift on M2, TPS47 and SAGA was 0.003°, 0.001° and 0.0003°C. Temperature precision on a given station was 0.001°C for all three cruises.

CTD and bottle salinity precision within each full cruise was 0.001 to 0.002‰. Accuracy is degraded because of Wormley standard seawater (SSW) batch differences. SSW batches P92, P96 and P103 were used on M2, TPS47 and SAGA, respectively. P92 is 0.003‰ higher than P96 (Mantyla, 1987), and P103 is 0.002‰ higher than P96 (A. Mantyla, personal communication). These differences were corroborated by deep salinity differences on geographically overlapping stations from the three cruises. We made a conscious decision to refer the salinities to the SSW for each cruise without additional shifts to some "standard" SSW because of drift in the differences between various SSWs (Mantyla,

1987), believing it more appropriate to simply state the SSW batch used for each cruise. Generally, investigators who wish to combine deep Pacific results from many cruises must take the SSW differences into account; unfortunately this is only possible with access to data reports. It is hoped that a more accurate standard will be available in the future.

Oxygen measurements were made by Winkler titration, with accuracies for M2, TPS47 and SAGA of 1% and station precision of 0.01 ml l^{-1}. Nutrient measurements, made on a Technicon autoanalyser, are accurate to 2–3%. Station precision for silica is 1%. Phosphate precision on TPS47 is closer to 2% than the desired 1%, due to recurring minor problems. On M2, a batch of rusty springs in the Niskin bottles caused faulty phosphate analyses at many depths through Sta. 21 and in one bottle used primarily at 4500 m for much of the rest of the cruise; all spurious values were deleted from the final data set. There were also some problems with the TPS47 nitrate precision prior to Sta. 63; values from Stas 38–57 may be too low by about 1%.

3. VERTICAL SECTIONS

Basic presentation of the TPS47, SAGA, and M2 data is made using the color plates included with this issue of *Deep-Sea Research*.

A. Potential temperature

The TPS47 potential temperature section shows the expected features of the subpolar North Pacific, with an extremely intense and shallow thermocline and a temperature minimum which is pronounced west of Sta. 60 (178°E) and weakly present to Sta. 63 (178°W). The coldest near-surface water (<0.9°C) was found in the temperature minimum at the western boundary on the SAGA section; this very fresh shelf water was inshore of and in the southward-flowing East Kamchatka Current. With the exception of Stas 41–43, where upper water properties had some subtropical influence, all TPS47 stations from 19 to 98 and the SAGA stations are classified as either western subarctic (temperature minimum) or eastern subarctic (no temperature minimum, intense halocline). Hence the zonal length scale for water masses on TPS47 is large, as expected, and clearly differentiated from the shorter meridional scales evident on M2. On M2, a significant and abrupt shift in upper water properties, as seen in θ/S diagrams, occurs every 3°–4° latitude, and is discussed in the last section.

The western end of TPS47 was located well within the perturbed region of the Oyashio and Kuroshio (KAWAI, 1972). This region is typically characterized by onshore and offshore "intrusions" of the Oyashio separated by a "Kuroshio" intrusion (warm-core ring); TPS47 occurred during a time when this structure was quite pronounced. The warm waters are not truly subtropical, but are a mixture formed north of the Kuroshio (KAWAI, 1972; HASUNUMA, 1978). Ten-day analyses of 100-m temperature prepared by the Japan Meteorological Association and based on XBT data show how variable this region is (Fig. 2). Based on all 1985 10-day JMA analyses, the warm intrusion at TPS47 first formed in April 1985 was deformed, detached and re-attached to the warm Kuroshio waters; by the end of 1985 the region of water warmer than 10°C was much more extensive than in August. Salinity, silica and velocity in this region are discussed in later sections.

Except in the upper 150 m, the overall pattern of temperature on TPS47 closely reflects the density (Section 3C), with isotherms east of Sta. 38 (near the turning point of the cruise track) sloping broadly downward to the east at all depths, indicating large-scale northward flow relative to the bottom. On M2, the broad eastward flow of the subtropical and subpolar gyres is clear with isotherms doming upwards to the north above 3000 m. The narrow, westward-flowing Alaska Current is evident close to the northern boundary. The striking thermocline undulations north of Hawaii described elsewhere (TALLEY and DESZOEKE, 1986) appear to be time-dependent.

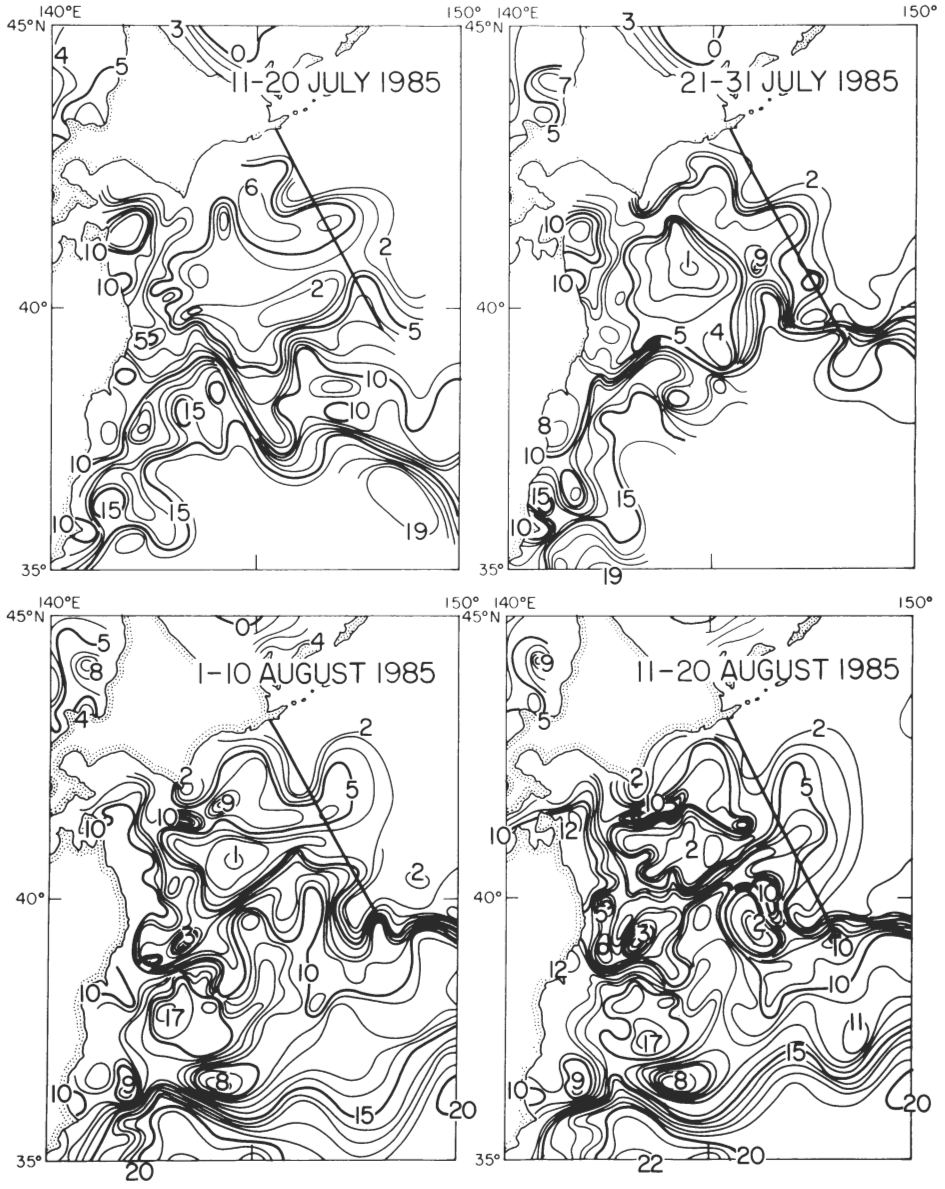

Fig. 2. Temperature at 100 m for 11–20 July, 21–31 July, 1–10 August and 11–20 August, 1985 from the Japan Meteorological Agency. Maps are based on all quickly available XBT temperature data. The TPS47 cruisetrack, which crossed this region from 5–9 August, is superimposed. The maximum 100 m temperature measured on TPS47 was 10°C, several degrees higher than observed in the XBT surveys.

On shorter zonal scales on TPS47, strong vertical coherence in isotherm slopes is evident visually at all locations between the western boundary and about 170°W. Right at the western boundary, changes of isotherm slopes are evident below 2200 m on SAGA and below 3500 m on TPS47. Similar slopes are also apparent at most depths at the northern boundary on M2. These may be transient phenomena or may reflect very narrow boundary currents inshore of the main boundary currents. (Associated silica anomalies are described in section 2E and may indicate permanence.)

Although not evident from the three vertical sections, the lowest abyssal potential temperature, slightly less than 1.05°C, was found at TPS47 Stas 12–13, 17 and 21–22 in the Kuril–Kamchatka Trench and over the Zenkevich Rise. The coldest abyssal water on SAGA was a barely undiminished 1.052°C at adjacent Stas 3 and 12 in the Trench. Abyssal water colder than 1.06°C was found at TPS47 Stas 8–24, over a 500 km range extending well east of the Trench; on SAGA, it was found in the Trench at Stas 2–4 and 12, a 60 km range; since the same Neil Brown CTD and calibration facility was used for both data sets, this narrowing is presumed to be real. WARREN and OWENS' (1988) map of temperature at 4000 m does not show an eastward "escape route" between our two sections for the coldest deep waters; hence the difference in amounts of the coldest abyssal water must be due to either recirculation or vertical mixing/upwelling. The coldest abyssal water on M2 is found in a broad band at the bottom north of the Hawaiian Ridge (<1.06°C at Stas 8–24) and in the Aleutian Trench. These are separated by older, warmer water which has been gently heated from below (JOYCE *et al.*, 1986).

At the eastern boundary (TPS47), the dynamic signature of the northward-flowing eastern boundary undercurrent beneath a southward surface current is apparent. At the ocean bottom near the eastern boundary, at the west end of the 2700-m deep Cascadia Basin, the isotherms plunge downward. This can be attributed to geothermal heating at the northern end of the Juan de Fuca Ridge.

B. Salinity

The TPS47 and SAGA salinity sections show the usual subpolar structure of monotonic increase with depth. On the late summer TPS47 section, both seasonal and permanent haloclines are apparent. The former is weak and associated with a strong seasonal thermocline. The only exception to the subpolar structure is the previously-mentioned subtropical water at TPS47 Stas 8–18 and 41–43. The former have a well-defined salinity minimum at about 300 m in the density range 26.6–26.8σ_θ; this is the only occurrence of North Pacific Intermediate Water (NPIW) on TPS47, whereas NPIW is obvious at all M2 stations south of 46°N. NPIW in the TPS47 stations is not a result of simply layering lower salinity subpolar and higher salinity subtropical waters: despite being a vertical salinity minimum, the NPIW is a salinity maximum along intersecting isopycnals (Fig. 3), indicating a strong subtropical influence even at the minimum.

As in the TPS47 temperature section, the TPS47 isohalines appear vertically coherent to the bottom west of 170°W. At the western boundary, the East Kamchatka Current is apparent on SAGA; the associated isohaline slopes extend to 3500 m. At the eastern boundary on TPS47, the upwelling and undercurrent signatures in the upper 400 m are pronounced.

M2 salinity structure varies from a strong halocline with monotonic increase with depth in the subpolar regime (north of 46°N), to solidly subtropical with nearly monotonic

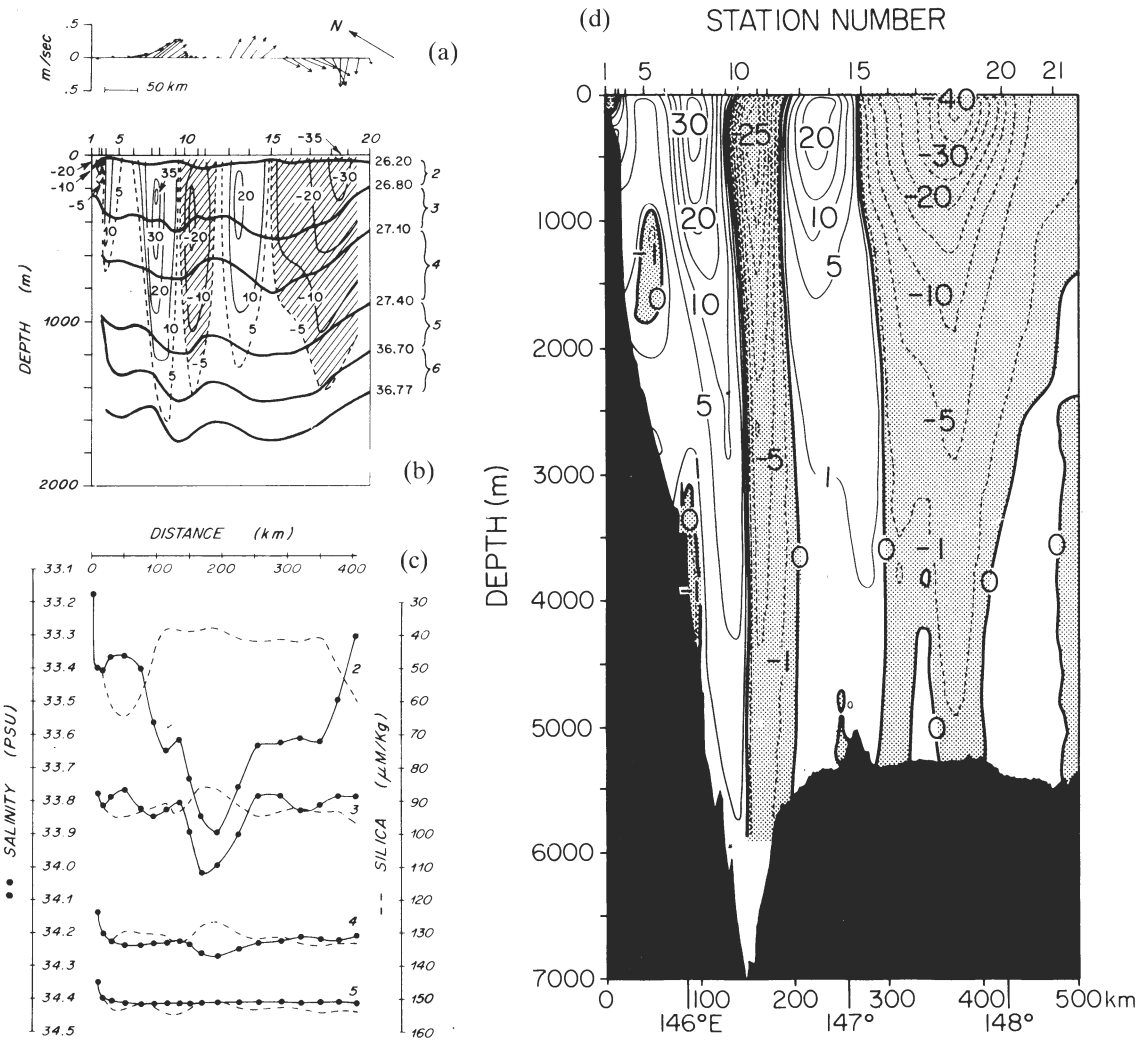

Fig. 3. TPS47 stations 1–20, across the Kuril-Kamchatka Trench: (a) 100 m ADCP velocities; (b) geostrophic velocity (cm s^{-1}) relative to 2000 dbar superimposed on potential density; (c) average salinity and silica for isopycnal layers 2, 3, 4, and 5 as shown in (b); (d) geostrophic velocity (cm s^{-1}), interpolated using Roemmich's (1983) objective mapping. Positive velocities are northeastward, perpendicular to the section.

increase both upward and downward from the NPIW south of 34°N. Between 34° and 46°N, salinity increases upward from the NPIW to a maximum at about 200 m, and then decreases to a minimum near the sea surface. Within this overall salinity maximum above the NPIW, there is also a second well-defined salinity minimum, which is not obvious in the vertical section; this is discussed in the last section.

Deepest salinities on the three sections agree well with Mantyla and Reid's (1983) bottom salinity, which is highest to the south with a tongue greater than 34.69‰ along the Aleutians. The M2 bottom salinities match their values, while an increase of TPS47 salinities by 0.003‰ would place the bottom values squarely in line. (While they did not adjust salinities used in their maps, Mantyla and Reid were aware of SSW batch variation and smoothed the contouring accordingly.) Within the broad saline tongue along the Aleutians, apparent in Mantyla and Reid's map, the new closely-spaced sections reveal that the highest salinity on a given crossing of the boundary is found in the bottom of the

Trenches. Corrected for SSW differences, little change is found in these highest salinities from section to section. The highest TPS47 and SAGA salinities are 34.690 and 34.691‰, respectively, with 34.688‰ salinities on TPS47 at about the same depth as 34.690‰ on SAGA, reflecting the 0.002‰ difference in SSWs. In the Aleutian Trench at 152°W, the highest M2 bottom salinity is about 34.690‰ (34.687‰ if adjusted to TPS47). This is barely changed from TPS47 given that the Aleutian Trench at 152°W is not as deep as the Kuril–Kamchatka Trench. Sections in 1982 at 175°E, 175°W and 165°W (WARREN and OWENS, 1988) show significantly higher deep salinities (>34.695‰ in the Trench bottom and >34.690‰ over a wide latitude range), but the discrepancy is probably due to SSW differences. (Warren and Owens' 1981 sections at 175°E and 175°W, using different SSWs and which are not shown in the cited paper, are consistent with the TPS47/SAGA data.) Thus, the Trench behaves as an active conduit of the saltiest abyssal water, with little apparent change in salinity along its extent. The source of high salinity water is to the south, based on MANTYLA and REID (1983), a section at 35°N (KENYON, 1983), and a section at 24°N (ROEMMICH *et al.*, 1991).

Comparing TPS47 deep isohalines in the eastern Pacific with deep isotherms, we find that both curve up to the east over the Cascadia Basin, and the deepest isohalines (34.67, 34.68‰) do not plunge into the bottom west of the Basin, unlike the isotherms. The latter observation suggests that geothermal heating is responsible for the bottom temperature/density behavior rather than boundary mixing; this topic is pursued in TALLEY and JOYCE (submitted).

C. *Potential density (σ_θ and σ_4)*

The overall potential distribution suggests broad northward flow across most of TPS47 and eastward flow above 300 m on M2. As noted for potential temperature and salinity, vertical coherence of the mesoscale features on TPS47 is visually high from top to bottom west of 170°W. The expected boundary currents (East Kamchatka on SAGA, Alaska on M2, a weaker southward eastern boundary current and a poleward undercurrent at the eastern boundary on TPS47) are also apparent. On M2 north of the Hawaiian Ridge, the strong undulations in density are most likely to be due to the presence of the Hawaiian Ridge (TALLEY and DESZOEKE, 1986). No single boundary current is found at the western boundary of TPS47 since the cruise track crossed the northern part of the mixed region between the Kuroshio and Oyashio, as discussed above. In the "subtropical intrusion" in this region, σ_θ is nearly as contorted as potential temperature and salinity; the implied velocity structure is narrow cyclonic flow (Stas 10–15) around the most intense subtropical water (Stas 12–13), flanked by a broad anticyclonic flow (Stas 2–22) in which the subtropical plug is embedded (Stas 8–18).

Across the tops of the SAGA and TPS47 sections and the subpolar part of M2 stretch the seasonal pycnocline and the thicker remnant of the winter mixed layer. The latter is marked by the temperature minimum at its core in the western Pacific and by the strong underlying halocline in the eastern Pacific. (The thickness of the winter remnant is artificially emphasized by the contour choices.) Apparent in the remnant winter mixed-layer is the progression from least dense in the east (25.5–26.0σ_θ) to densest in the west (26.6σ_θ on SAGA), which is so evident in winter surface density maps (REID, 1969).

At mid-depth at the western boundary on SAGA and TPS47 and at the northern boundary on M2, the sharp reversal of isotherm slopes is accompanied by similar isopycnal

behavior. Similar sharp reversals are apparent on other closely-spaced boundary sections, for instance, the 28°S/43°S sections (STOMMEL *et al.*, 1973).

Other noteworthy features of the σ_4 section are: (1) the upward isopycnal slopes on TPS47 over the Cascadia Basin compared with the downward slopes on the offshore side of the ledge; (2) deep isopycnals on TPS47 which plunge downward within about 400 m of the bottom in the eastern Pacific, mirroring the deep isotherms; (3) high density just north of the Hawaiian Ridge on M2; and (4) the discontinuities on TPS47 across the Emperor Seamounts, due to salinity discontinuities. The last effect is real and reflects confinement of the densest, most saline abyssal waters to the region west of the Seamounts. At mid-depth, the densest water is east of the Seamounts. The gaps in the Seamounts deeper than 5000 m and nearest to TPS47 are in two broad regions, near 39°N and 54°N; thus, the path between the two sides of the Seamounts is at least 2000 km long. RODEN and TAFT's (1985) data in the 39°N gap match values west of the Seamounts on TPS47.

The very densest water on TPS47 and SAGA occurs in Kuril–Kamchatka Trench. The apparently lower value at TPS47 is due entirely to the salinity accuracy described in Section 2C; the densest water on both sections is the same. Based on abyssal maps (MANTYLA and REID, 1983) and the 24°N section (ROEMMICH *et al.*, 1991), the source of densest bottom water lies to the south. Thus, the deepest water in the Trench may be flowing northwards. The bottom water in the Aleutian Trench on M2 must come from the west along the boundaries.

D. Oxygen (ml l^{-1})

All three sections show the familiar high oxygen surface layer, an oxycline coinciding with the permanent pycnocline, a decrease to a minimum at 500–1000 m, and a gradual rise toward the ocean bottom. Most TPS47 and SAGA surface values exceed 110% saturation, calculated with respect to *in situ* temperature, with the highest, in excess of 135%, at SAGA coastal Stas 5, 6 and 9. Even when saturation is computed with respect to the freezing point temperature, surface waters on all three cruises are still supersaturated. This contrasts with REID's (1982a) observations in the northern North Pacific, where he found undersaturated winter surface waters.

The lowest oxygen measured on TPS47 was 0.21 ml l^{-1}, with a well-defined region of less than 0.25 ml l^{-1} in the oxygen minimum east of 130°W (Fig. 4); this is lower than shown in published maps near the oxygen minimum (e.g. REID, 1965; REID and MANTYLA, 1978). At 152°W, the core of oxygen lower than 0.25 ml l^{-1} occurs between 30° and 42°N (Fig. 5b) and reflects a tongue of the lowest oxygen at the oxygen minimum extending southwestward from the eastern boundary, shown in the same references. Reid and Mantyla's dynamic topography at 1000 dbar relative to 3500 dbar shows anticyclonic circulation at 47°N east of 180°N with the gyre axis trending from southwest to northeast. The southwestward branch of their anticyclonic flow in the eastern Pacific occurs where oxygen in the oxygen minimum is laterally lowest. ROEMMICH and MCCALLISTER's (1989) inverse calculation of M2 velocities also indicates westward flow at the oxygen minimum between 30° and 42°N.

On the TPS47 vertical section and in Fig. 4b, oxygen at the minimum is also seen to be relatively low between 155°E and 180°. (A similar feature is seen at the phosphate and nitrate maxima.) Is this western low oxygen distinct from that near the eastern boundary? Two possible avenues of connection from east to west are along the tongue of low oxygen

between 30° and 42°N described in the previous paragraph and along the Alaska Current. Connection from west to east would be via the eastward flow in the southern subpolar and northern subtropical gyre. REID and MANTYLA's (1978) map of oxygen at $32.0\sigma_1$ shows separate regions of low oxygen in both the Bering Sea and near the eastern boundary. They show the mid-latitude tongue extending southwestward as part of the anticyclonic gyre, hence with no connection to the Emperor Seamounts region at 47°N, which lies

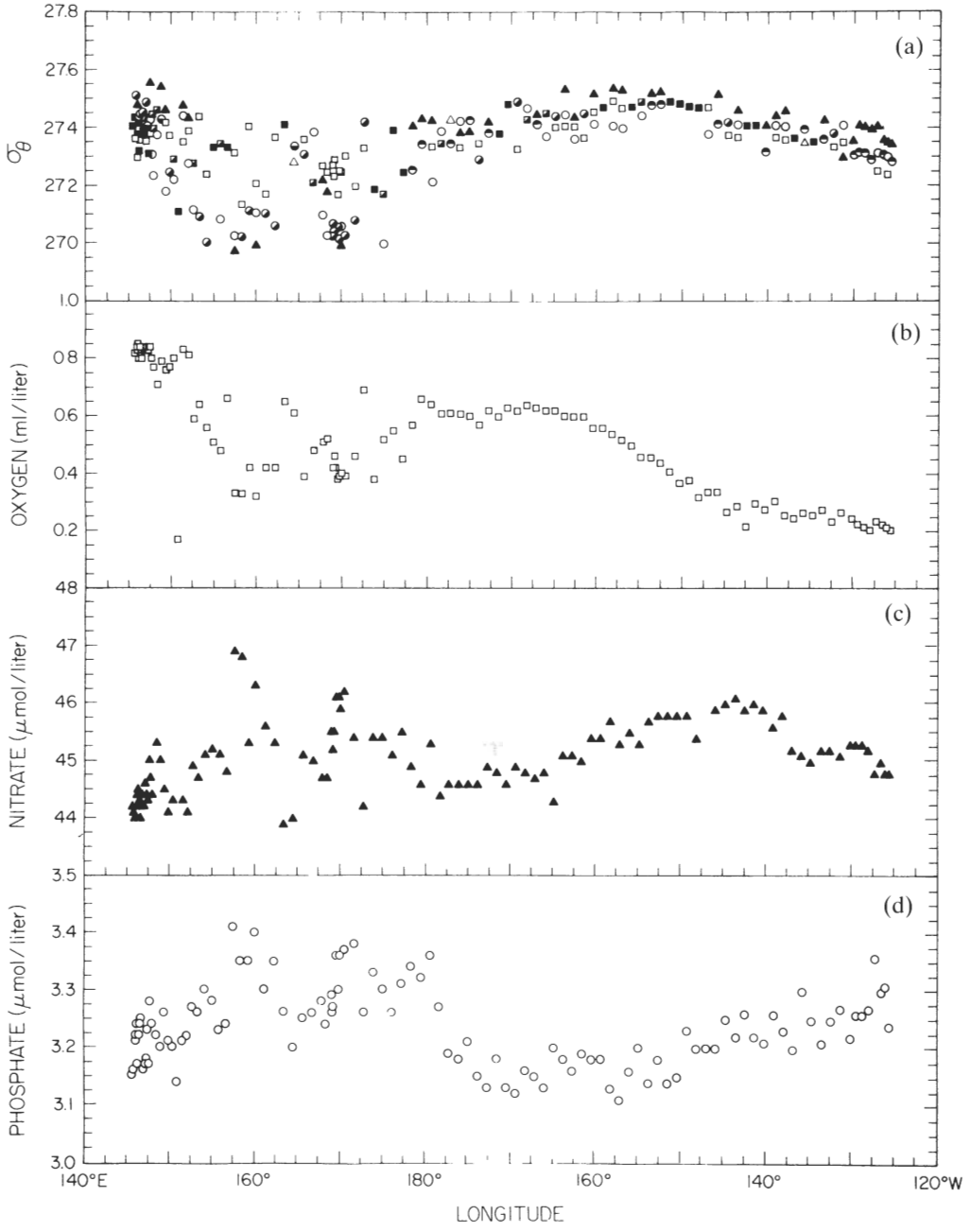

Fig. 4. (a) Potential density (σ_θ) at the oxygen minimum (open squares), nitrate maximum (shaded triangles) and phosphate maximum (open circles). Coincident points are indicated by partially shaded circles and squares. (b) Oxygen (ml l^{-1}), (c) nitrate (μmol l^{-1}), and (d) phosphate (μmol l^{-1}) at their respective extrema along TPS47, with no interpolation of the Niskin data.

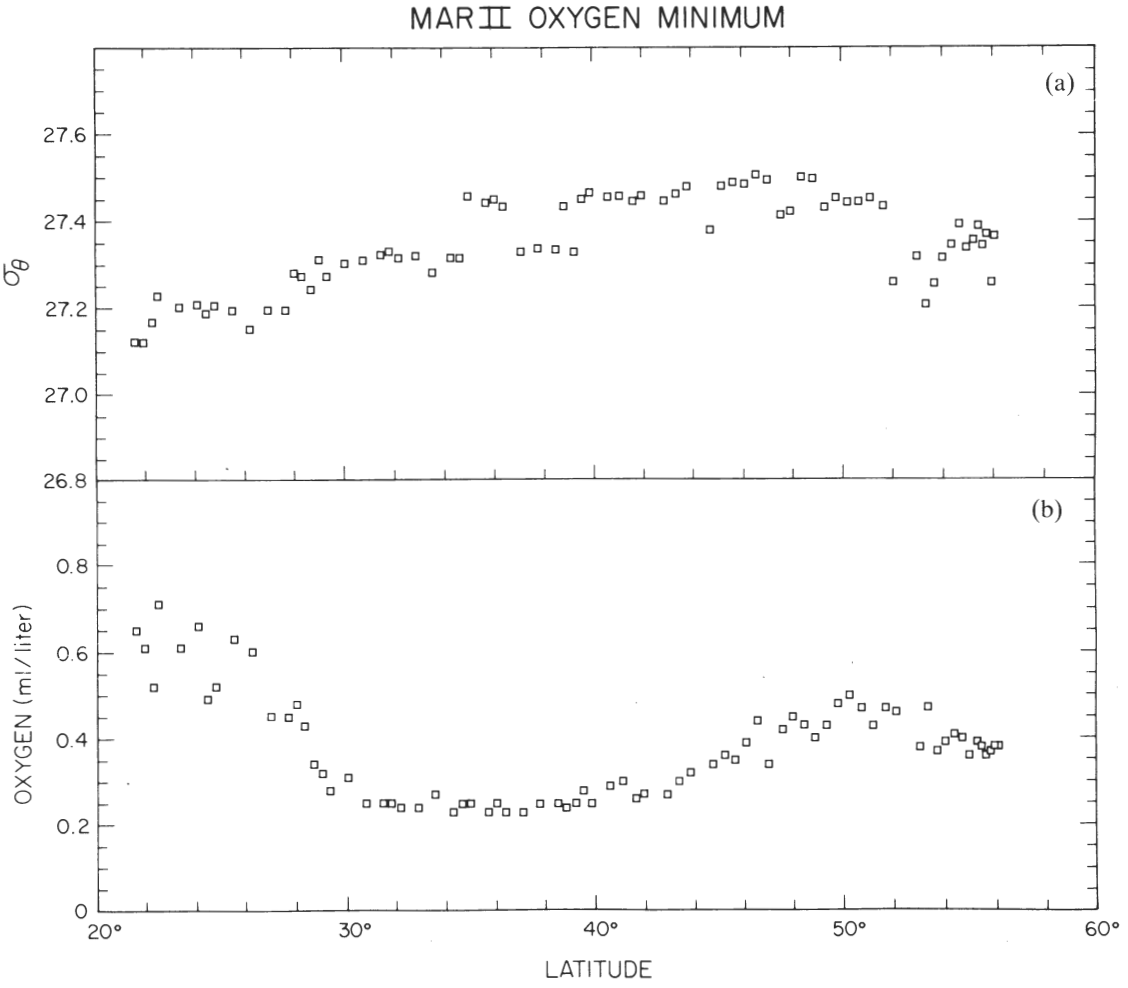

Fig. 5. (a) Potential density (σ_θ) and (b) oxygen (ml l^{-1}) at the oxygen minimum along 152°W. No interpolation of the discrete Niskin data was used.

within a wholly-enclosed cyclonic circulation shown on their 1000/3500 dbar topography. They also show no connection of the low oxygen in the Alaska Current in the Gulf of Alaska with the low oxygen in the Bering Sea and western subpolar gyre.

The substantial new data sets collected in the 1980s result in little change to REID and MANTYLA's (1978) oxygen distribution; a section at 175°W in 1984 (JOYCE, 1987) shows that the mid-latitude tongue of oxygen less than 0.5 ml l^{-1} does not extend westward across this longitude and therefore cannot feed the western subpolar gyre. Oxygen at the minimum was discussed by WARREN and OWENS (1988) for their closely-spaced sections across the Aleutian Trench at 165°W, 175°W and 175°E; they reported that the lowest oxygen, while lying in the westward-flowing Alaska Current, is separated from the Aleutian Islands by a band of higher oxygen in the swifter part of the current. [This feature was not found on the M2 section (Fig. 5b), where low oxygen persists to the northern boundary.] With Warren and Owens' sections, low oxygen cannot be contoured between the eastern and western Pacific, suggesting no connection along either the Alaska Current or the eastward flow to the immediate south. However, additional historical data available in the full NODC data set in the Alaska Current show that there could be a continuous tongue of low oxygen along the Alaska Current and do not rule out a northeast Pacific source for the 0.5 ml l^{-1}

oxygen near the Emperor Seamounts at 47°N. On the other hand, oxygen lower than 0.4 ml l^{-1} is found close by on TPS47 nearer Kamchatka; this cannot be connected in any way with the northeast Pacific. The Bering Sea and East Kamchatka Current, along with continual consumption, seem to be the most likely sources of the low oxygen found in the western portion of TPS47, with both oxygen and salinity patterns matching Reid and Mantyla's 1000 dbar circulation well. (Salinity at $32.0\sigma_1$ in this portion of the subpolar gyre is not greatly different from the Bering Sea.)

In the deep water east of the Emperor Seamounts, oxygen contours bend to intersect the bottom, although the exact slope is uncertain since measurement precision is 1%. Oxygen on deep isopycnals along TPS47 (Fig. 6b) is depleted at the eastern boundary, suggesting that oxygen intersects the bottom more steeply than density within 300 m of the bottom.

Highest oxygen in the deep water is found in the Kuril–Kamchatka Trench, exceeding 3.75 ml l^{-1}; this water must have come from the south. The relative amount of highest oxygen suggests a slightly smaller volume of this water at SAGA relative to TPS47. Oxygen in the Aleutian Trench on M2 is greater than 3.5 ml l^{-1}. Combining the three sections with those of WARREN and OWENS (1988) in the Aleutian Trench, the oxygen distribution indicates northward and eastward aging below the trench "lip" depth. Bottom oxygen higher than 3.75 ml l^{-1} is also found north of the Hawaiian Ridge, in a region where all properties indicate a southern source (JOYCE *et al.*, 1986).

E. Silica (μmol l^{-1})

Silica sections show the expected very low surface values, increasing to an intermediate maximum (1500–2500 m) and then decreasing downward. A well-defined bottom maximum is also found in the eastern Pacific. The intermediate depth maximum is well-known and found throughout the North Pacific (e.g. EDMOND *et al.*, 1979). On the other hand, the M2 and TPS47 observations are the first large group of measurements of the bottom maximum—prior observations were restricted to a few GEOSECS stations (CRAIG *et al.*, 1981). Highest silica overall is found just at the bottom of Cascadia Basin, with values exceeding 200 μmol l^{-1} in a density range appropriate for the intermediate maximum offshore of the Basin. Along 152°W the most extreme silica values in the intermediate maximum are confined between 40° and 52°N except in an extremely narrow band at the northern boundary beneath the Alaska Current, suggesting westward flow from a northeast Pacific source down to a depth of 3000 m. While separation between western and eastern high silicas at the maximum on TPS47 is less pronounced than between separate regions of the shallower oxygen minimum, there is a similarity in patterns, which is more obvious on the isopycnal plots (Fig. 6). Low oxygen near the Emperor Seamounts appears to have come from the Bering Sea and/or local consumption. In TALLEY and JOYCE (submitted) we show that the high silica probably has a local origin.

At the western boundary, SAGA and TPS47 reveal very narrow bands of high silica, suggesting southward flow at 1500–2000 m from a northern source. The sources of the intermediate and bottom silica maxima are discussed in greater detail in TALLEY and JOYCE (submitted).

The brokenness of the intermediate silica maximum in the eastern Pacific at a level of less than 5 μmol l^{-1} may not be realistic. Since silica precision within a station is 1% and accuracy within the cruise is 2–3%, this level of fluctuation is nearly within the measurement error.

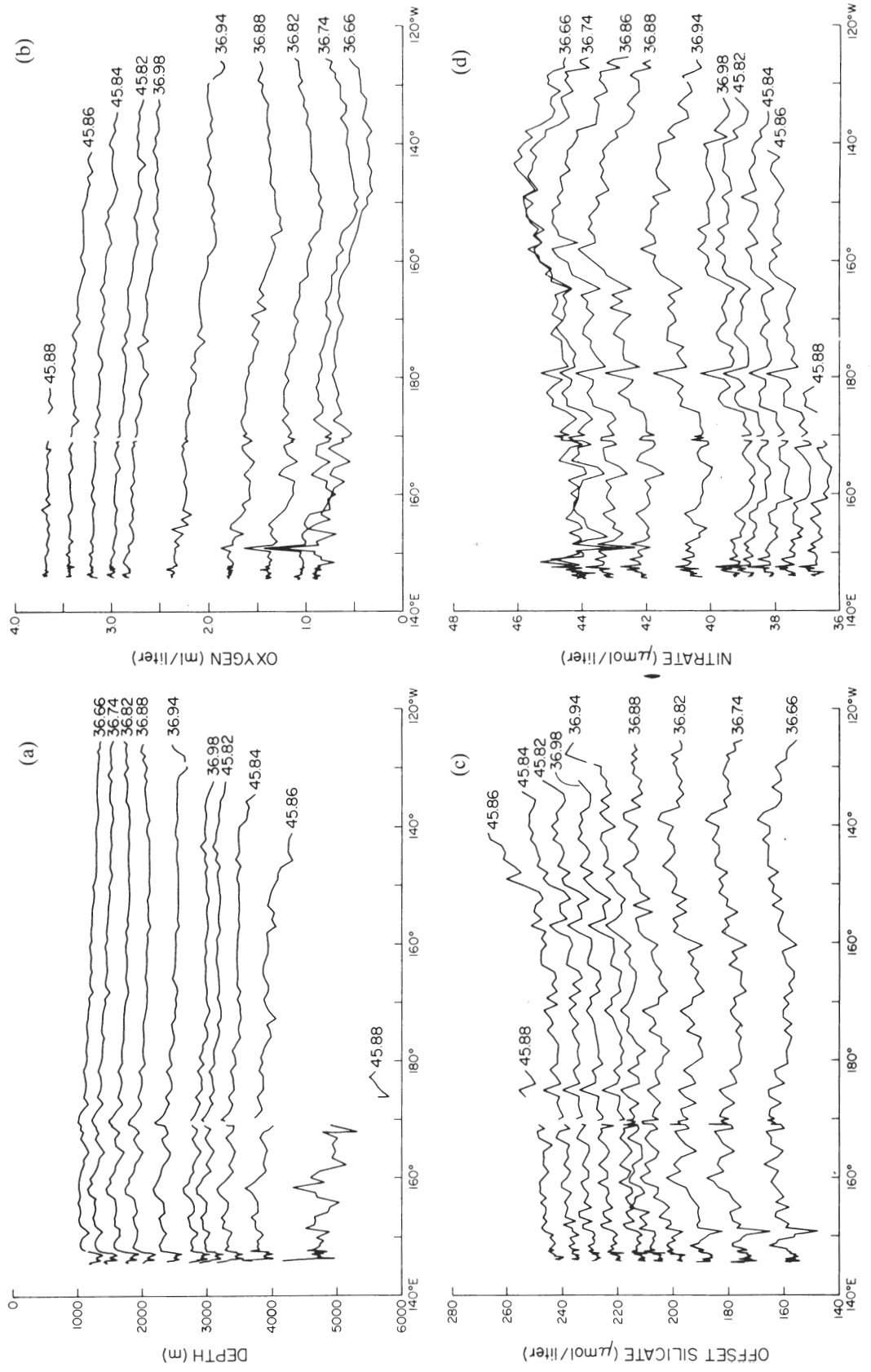

Fig. 6. (a) Depth of several σ_2 (36.66–36.94) and σ_4 (45.82–45.88) isopycnals along TPS47. (b) Oxygen (ml l^{-1}), (c) silica (μmol l^{-1}) and (d) nitrate (μmol l^{-1}) on the same isopycnals. Silica is correct for 36.66 σ_2; each trace thereafter is offset by +10 μmol l^{-1} from the previous isopycnal. Values were obtained using a cubic spline interpolation to 10 m depths followed by linear interpolation to the desired isopycnals.

Also of note is low silica, relative to adjacent bottom waters, at the bottom of the Kuril–Kamchakta Trench on TPS47 (145 μmol l^{-1}) and SAGA (152 μmol l^{-1}), and in the Aleutian Trench on M2 (160 μmol l^{-1}). On TPS47, the region of 155 μmol l^{-1} silica extends up to 4000 m and across the entire first "dogleg" to Sta. 25, indicating southern influence from the bottom up to at least 4000 m. The increase from TPS47 to SAGA is marginally greater than the measurement error and reflects northward flow in the trench. On M2, low silica in the Aleutian Trench relative to the rest of the section indicates a western source based on isopycnal analysis (TALLEY and JOYCE, submitted). The increase in silica to the north and east along the boundaries results from the bottom source of silica—other properties, such as salinity, which have no deep source or sink are more nearly conserved. Abyssal silica values less than 155 μmol l^{-1} are found broadly banked north of the Hawaiian Ridge on M2, also suggesting a southern source.

F. Phosphate and nitrate (μmol l^{-1})

The phosphate and nitrate vertical sections show the expected low surface values and intermediate-depth maxima, coinciding roughly with the oxygen minimum (Fig. 4). Highest phosphate and nitrate at the maximum are found in the east and in a separate region around the Emperor Seamounts, mirroring the oxygen minimum structure. Near the eastern boundary, nitrate at the maximum becomes depleted relative to phosphate, whose maximum is much closer to the boundary. ROEMMICH *et al.* (1991) have reported a similar eastern boundary effect on TPS47 due to denitrification (GOERING, 1968). There is also a shift in the N:P ratio at mid-depth at about 180° with relatively higher phosphate to the west, but this may be linked to analytical problems for nitrate. On deep isopycnals, nitrate (Fig. 6d) increases towards the east between 165°E and 160°W but not as monotonically as oxygen decreases (Fig. 6b). The deep phosphate distribution on isopycnals is similar to nitrate. Nitrate and phosphate are both high near 180°, unmatched by oxygen.

Deep phosphate and nitrate in the Kuril–Kamchatka Trench are low on TPS47 and SAGA, with nearly no change between sections. On M2, values at the bottom of the Aleutian Trench are essentially the same as at the western boundary; since low phosphate and nitrate indicate a southern source, the measurements corroborate the suggestion, based on other properties, of northward and eastward flow at the bottom of the Trenches. At the bottom north of the Hawaiian Ridge, low phosphate and nitrate also indicate a southern source, in accord with other properties.

4. DISCUSSION

Earlier papers using these data examined the effect of slow geothermal heating on the abyssal temperature and density, showing a region of warmest water in the north Pacific (JOYCE *et al.*, 1986), and the set of strong currents in the upper water north of the Hawaiian Ridge (TALLEY and DESZOEKE, 1986). An accompanying paper (TALLEY, 1991) treats the source of a single station $\theta/S/O_2$ anomaly near the Kuril Islands on TPS47; the anomaly, at 27.4 σ_θ, is shown to have originated in the Okhotsk Sea and provides the basis for a discussion of water mass modification in the North Pacific at densities of 26.8–27.6 σ_θ. The double silica maximum is discussed in much greater detail in TALLEY and JOYCE (submitted).

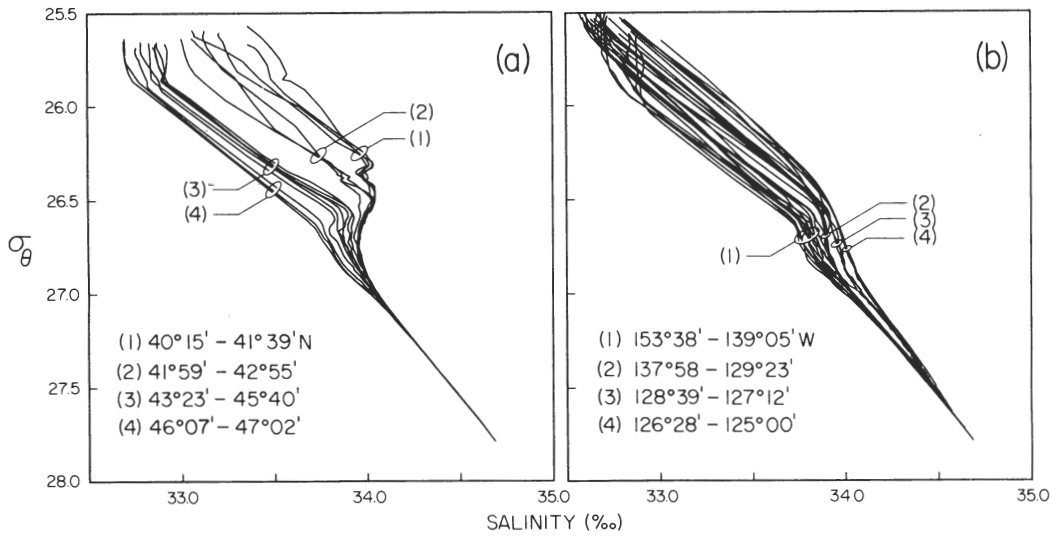

Fig. 7. (a) Potential density vs salinity from M2 (152°W), with a jump south and north of the Subarctic Frontal Zone, located between 42° and 43°N, and showing eroded NPIW as far north as 46°N where another front occurs. Circles indicate station groups. (b) Potential density vs salinity from TPS47, showing a region of eroded NPIW between 138° and 129°W and warmer waters over the Cascadia Basin. Zonal changes in σ_θ/S along TPS47 are generally more continuous than meridional changes along M2.

Upper water properties on TPS47 and M2 suggest that the split between subtropical and subpolar circulation in the eastern Pacific is somewhat ambiguous. Potential density vs salinity from M2 (Fig. 7a) shows the Subarctic Frontal Zone at 42°–43°N, separating surface waters with a sharp shallow salinity minimum from purely subpolar waters which have a simpler, intense halocline. The frontal zone is a few degrees south of the zero of annual-averaged Sverdrup transport (approximately 45°–50°N from HELLERMAN and ROSENSTEIN, 1983; 46°N from TALLEY, 1985). South of the Subarctic Front, the North Pacific Intermediate Water (NPIW), recognizable as a rounded salinity minimum at about 26.7 σ_θ with an overlying salinity maximum, is strong and varies little through the station group. However, *north* of the Subarctic Front up to 46°N is also found an eroded version of NPIW. Well-defined NPIW is characteristic of the subtropical gyre; its eroded presence between 43° and 46°N suggests a leaky gyre boundary or that the boundary is closer to the latitude of zero-averaged Sverdrup transport than is the Subarctic Front. Along TPS47, NPIW with an overlying salinity maximum is not found, but there is a distinct plateau in σ_θ/S between 138° and 129°W ending at the western edge of the Cascadia Basin. All surface waters west of this on TPS47 are subpolar and correspond in potential density/salinity with waters north of the 46°N break along 152°W. This suggests that NPIW advects into the subpolar gyre where its overlying salinity maximum is eroded. In the Cascadia Basin on TPS47, all waters with a density less than about 27.6 σ_θ are more saline, hence warmer, than offshore waters, which may result from local processes (e.g. hydrothermal venting). Finally, abrupt changes in upper ocean σ_θ/S along M2 contrast with more gradual changes along TPS47. While station separation is closer on M2 so that changes might be better sampled than along TPS47, the overall envelope of profiles for the two is similar; a decimated version of M2 does not look like TPS47.

Along 152°W at 1000 m, which is within the wind-driven circulation, the oxygen minimum's density and strength (Fig. 5) indicate a northward shift of the demarcation

between eastward and westward flow with depth in the subtropical gyre. This is related to the poleward shift of the gyre center as noted by REID and MANTYLA (1978). Westward flow at the oxygen minimum, assuming advection of low oxygen from the eastern boundary, is found between 30° and 42°N, with eastward flow of relatively higher oxygen extending northward to about 52°N. Thus the subtropical gyre center appears to shift from 25°N at the surface (WYRTKI, 1975) to about 40°N at 1000 dbar, as suggested in REID and MANTYLA's (1978) Figure 4.

Two complementary approaches to the intermediate and deep water property distributions are to examine properties at their well-defined vertical extrema (Figs 4 and 5) and along isopycnals (Fig. 6). Only the nitrate/phosphate maxima and oxygen minimum from TPS47 are shown in Fig. 6; the silica maximum is considered by TALLEY and JOYCE (submitted). The oxygen minimum from M2 is shown in Fig. 5. The near-coincidence of the nitrate, phosphate and oxygen extrema is well-known and is due to similar biological processes. The density of all three extrema (Figs 4a and 5a) lies between 27.0 and 27.55 σ_θ (used rather than σ_1 for easy correspondence with the vertical sections). The depth as seen in the vertical sections ranges from 200 m in the west to 1500 m in the east and at the western boundary along TPS47. As discussed in Section 3D, two distinct geographical regimes are apparent in all extrema and also in their density and depth, divided roughly at 180°. In the west, the properties, density and depth are scattered, with the lowest density and shallowest occurrences on the section. East of 180°, all properties are much smoother, with a clear trend to "older" water (lower oxygen, higher nitrate and phosphate) towards the east. The "newest" water is found just east of 180° and at the western boundary, off Hokkaido. These patterns suggest the subpolar circulation shown, for instance, in REID and MANTYLA (1978) for 1000 dbar, with an enclosed cyclonic gyre west of 180°, an elongated cyclonic gyre stretching all along the Aleutians enclosing the western gyre, and an anticyclonic gyre tilted southwest–northeast with its axis shifted well north in the eastern Pacific relative to its surface expression. The demarcation in properties at mid-depth at 180° on TPS47 (Fig. 4) corresponds roughly with REID and MANTYLA's (1978) "separation streamline" between the cyclonic and anticyclonic circulations. The anticyclonic circulation advects newer water into the eastern Pacific and returns oxygen-poor water to the west between 30° and 42°N.

On σ_2 and σ_4 isopycnals from TPS47 (Fig. 6), oxygen, nitrate and silicate all exhibit trends indicating older water to the east, as expected from past studies. Phosphate is not shown because of accuracy problems. On σ_4s, which lie below 3000 m, nitrate has a minimum near 160°E. On σ_2s, lying between 1000 and 3000 m, the large-scale trends of oxygen and nitrate are similar west of the Emperor Seamounts (170°E) and approximately opposite to the east—the latter is the expected behavior if similar sources and biological processes were found throughout. Silica trends are similar to oxygen up through the silica maximum at about 36.9 σ_2, above which silica flattens owing to the lack of a silica source on the shallower isopycnals. Both oxygen and silica change precipitously on some σ_2s at the eastern boundary, due to hydrothermal venting (TALLEY and JOYCE, submitted). All three properties have a lateral extremum between 160° and 140°E, indicating older waters. This rather broad "detail" is only apparent on isopycnals lying between 1000 and 2000 m, so does not appear on REID and MANTYLA's (1978) maps near 1000 m or on REID's (1982b) maps near 2500 m.

We have noted in discussing the vertical sections the indications of abyssal flow direction in the Kuril–Kamchatka and Aleutian Trenches and north of the Hawaiian Ridge. Prior to

the three cruises discussed in this paper, no detailed crossings of the western boundary trenches were available. WARREN and OWENS' (1985, 1988) measurements across the Aleutian Trench at 175°E, 175°W and 165°W corroborated REED's (1969) suggestion, based on limited hydrographic data, of eastward bottom flow in and just south of the Aleutian Trench. They also found intense westward flow down to 3000 m on the northern side of the trench and interpreted the complex of boundary currents using a modified STOMMEL and ARONS (1960) model of abyssal flow. In the absence of direct current measurements on our three subarctic sections, flow direction can only be inferred from property distributions and geostrophic shear. At TPS47 and SAGA stations located directly in the Kamchatka Trench, all properties below 4500 m indicate a southern source and hence northward flow (low potential temperature, silica, phosphate and nitrate; high salinity, density and oxygen with the appropriate changes from 42° to 49°N to indicate northward flow). Deep properties in the Aleutian Trench, including WARREN and OWENS' (1988) sections, are less extreme than at the western boundary, indicating a southwestern source of the deepest water in the Trench. The westward boundary current identified by Warren and Owens is evident at the silica maximum at intermediate depth (about 2000 m) at 152°W, indicating a narrow boundary flow (about two stations wide). Similar extremely narrow boundary currents are apparent at the western end of the TPS47 and SAGA sections and suggest southward flow.

While water properties indicate a general sense of intermediate and deep mean flow direction in the trenches, geostrophic velocity is more difficult to interpret because of the reference level uncertainty and time dependence. Geostrophic velocity relative to 2000 dbar at the western end of TPS47 with the ADCP velocities at 100 m juxtaposed (Fig. 3a,b) shows intense cyclonic flow surrounding the warm, saline intrusion, due to doming isopycnals below 200 m. The ADCP velocities, which correspond best with the 21–31 July temperature map (Fig. 2), confirm only the positive geostrophic velocities inshore of Sta. 15 and the far-offshore negative velocity. The eastward ADCP velocities close to shore reflect anticyclonic flow around the warm intrusion; the absence of the negative velocities seen in the geostrophic section between Stas 10–13 makes the whole warm water pool part of a larger anticyclone. The eastward flow farther offshore (Stas 13–14) may be part of the Oyashio front. Particularly important is the extension to the bottom of isopycnal slopes beneath the warm intrusion, which suggests that topographic steering may be an important component of the formation, location and movement of intrusions. Moreover, the high temporal variability observed at the surface may extend to the ocean bottom here.

Geostrophic velocity was calculated for the first 20 stations of TPS47 (Fig. 3d); a bottom level-of-no-motion in the Kuril–Kamchatka Trench and over the Zenevich Rise produces satisfactory results based on properties at deep levels. [ROEMMICH and MCCALLISTER's (1989) smoothed inverse solution shows northward bottom velocities of order 1 cm s^{-1} throughout this region and broad northward flow throughout the deep water.] The bottom-referenced flow is northwards in the center and west side in the Trench, southwards on the east side in the Trench, and weakly northwards on the rise east of the Trench. Narrow cells of southward flow along the western boundary match the property anomalies there. If, however, the ADCP velocities (Fig. 3a) yield a truer geostrophic circulation at 100 m than a bottom reference level calculation or Roemmich and McCallister's inverse, positive flow of 10–15 cm s^{-1} would be added to the negative flow cell over the eastern flank of the Trench. This would result in northeastward flow at all depths, with deep geostrophic velocities which seem too large to be likely in this region.

Equally troublesome and perhaps part of the difficulty with applying the ADCP measurements is the strong time dependence, which might overwhelm the mean flows apparent in tracer patterns.

We thus conclude, from the tracer distribution, that there is net northward flow near the bottom at the western boundary on TPS47 and SAGA and that the southward flow apparent in the geostrophic velocities may be due to time dependence, as is the amplitude of northward flow. At the western boundary, the bottom reference level produces two cells of southward flow that do not coincide with the isolated silica maximum at 1000–2000 m, which was interpreted as being due to southward flow. Particular care with choice of a reference velocity will be necessary in further calculations. With respect to abyssal circulation models (STOMMEL and ARONS, 1960; WARREN and OWENS, 1985), such trench flow has not been modelled, but seems consistent with a basic southern source, a very restricted pathway, and upwelling and mixing as the trench shoals around the northern boundary.

The Emperor Seamounts are a major topographic barrier to abyssal flow but no anomalies at the ocean bottom are evident near them on TPS47 in the color plates or in plots of properties on deep isopycnals (Fig. 6)—rather, there is a general change in deep isopycnal properties broadly indicating older water to the east. The disjuncture in depths of isopycnals below the seamount peaks on TPS47 (at about 170°E) reflects the nearly 3000 km separating the two sides through gaps in the Seamounts without a change in isopycnal properties.

Just north of the Hawaiian Ridge, all bottom properties are anomalous in a band between 25° and 30°N, indicating a southern source, just as on the western and northern

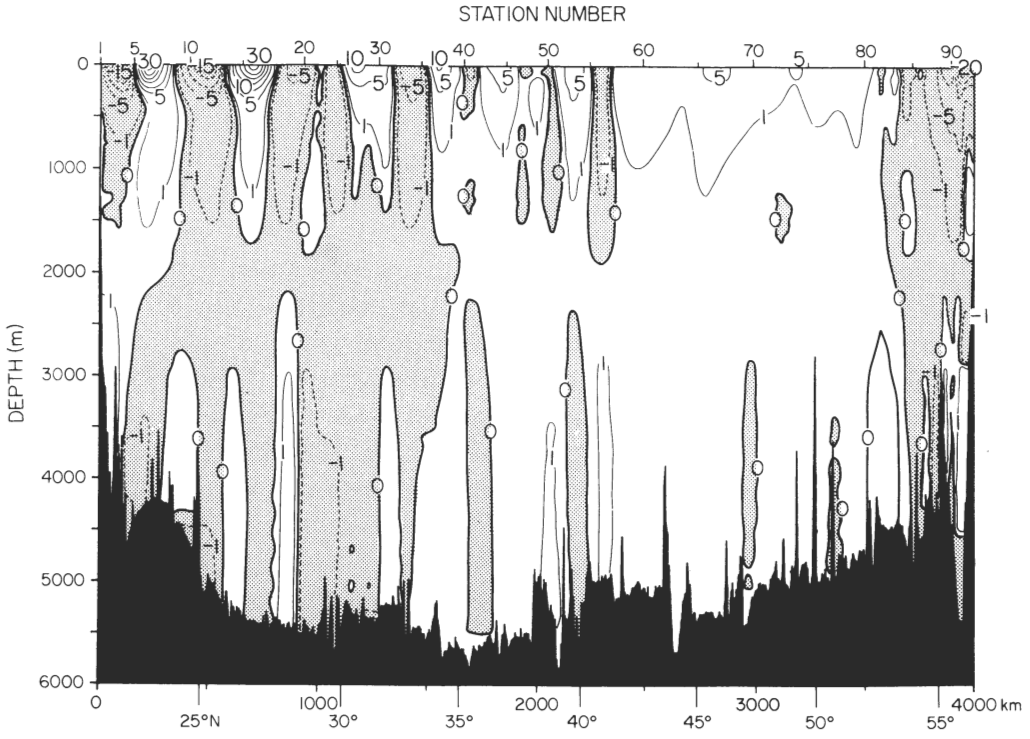

Fig. 8. Geostrophic velocity (cm s^{-1}) along M2 (152°W). ROEMMICH and MCCALISTER's (1989) smoothed 1000 dbar velocity, calculated from an inverse model, was used as the reference velocity. Positive velocity is eastward.

boundary sections. Geostrophic velocity (Fig. 8) was calculated for each pair of deep stations from M2 by referencing deep station pair velocities to 1000 m, gridding these to 10 km spacing and then re-referencing using ROEMMICH and MCCALLISTER's (1989) geostrophic velocity. The latter was calculated in an inverse model of the North Pacific and has a lateral smoothing scale which is much larger than the station pair separations; because the inverse conserves mass in deep layers, the smoothed reference velocity is a better choice than an arbitrary level surface of no motion. Bottom velocities on the broad slope north of the Hawaiian Ridge (out to 1000 km) are more complicated than the simple tracer extrema suggest, but this region of enhanced velocity corresponds to the most extreme anomalies in tracers. Westward deep flow stronger than 1 cm s^{-1} is seen in several patches separated by eastward flow, all embedded in generally westward flow. EDMOND *et al.* (1971) reported abyssal flow from Wake Passage rounding the eastern end of the Hawaiian Ridge; we may be seeing the continuation of this flow. The southern source of the abyssal waters north of the Hawaiian Ridge was also shown in JOYCE *et al.* (1986) using the M2 data.

Acknowledgements—This work was made possible by the excellent efforts of the Oceanographic Data Facility at Scripps Institution of Oceanography and the captains and crews of the R.V. *T. Thompson* (TPS47), the *Akademik Korolev* (SAGA II) and the R.V. *T. Washington* (MARATHON II). Data collection during SAGA II was made possible by Drs Valentin Koropalov and Richard Gammon of the Institute of Applied Geophysics in Moscow and the Pacific Marine Environmental Laboratory of the National Oceanic and Atmospheric Administration, respectively. We had helpful discussions with J. Reid, M. Martin, J. Baker and M. Denham provided computing assistance. The color plates were prepared by N. Hulbirt, F. Crowe and Arts & Crafts Press. The work was supported by the National Science Foundation, Ocean Sciences Division, by Grants OCE84-16211, OCE87-40379 and OCE86-58120 to Scripps Institution of Oceanography, by Grant OCE84-16197 to Woods Hole Oceanographic Institution, by Grant OCE83-16930 to Oregon State University, and by the Office of Naval Research through Contract N00014-84-C0218 to Oregon State University.

REFERENCES

CRAIG H., W. S. BROECKER and D. SPENCER (1981) GEOSECS Pacific Expedition, Vol. 4, Sections and Profiles, U.S. Government Printing Office, 251 pp.

EDMOND J. M., Y. CHUNG and J. G. SCLATER (1971) Pacific bottom water: penetration east around Hawaii. *Journal of Geophysical Research*, **76**, 8089–8097.

EDMOND J. M., S. S. JACOBS, A. L. GORDON, A. W. MANTYLA and R. F. WEISS (1979) Water column anomalies in dissolved silica over opaline pelagic sediments and the origin of the deep silica maximum. *Journal of Geophysical Research*, **84**, 7809–7826.

GOERING S. (1968) Denitrification in the oxygen minimum layer of the eastern tropical Pacific Ocean. *Deep-Sea Research*, **15**, 157–164.

HASUNUMA K. (1978) Formation of the intermediate salinity minimum in the northwestern Pacific Ocean. *Bulletin of the Ocean Research Institute University of Tokyo*, **9**, 47 pp.

HELLERMAN S. and M. ROSENSTEIN (1983) Normal monthly wind stress over the World Ocean with error estimates. *Journal of Physical Oceanography*, **13**, 1093–1104.

JOYCE T. M. (1987) Hydrographic sections across the Kuroshio extension at 165°E and 175°W. *Deep-Sea Research*, **34**, 1331–1352.

JOYCE T. M., B. A. WARREN and L. D. TALLEY (1986) The geothermal heating of the abyssal subarctic Pacific Ocean. *Deep-Sea Research* **33**, 1003–1015.

KAWAI H. (1972) Hydrography of the Kuroshio Extension. In: *Kuroshio: Physical Aspects of the Japan Current*, H. STOMMEL and K. YOSHIDA, editors, University of Washington Press, Seattle, pp. 235–352.

KENYON K. (1983) Sections along 35°N in the Pacific. *Deep-Sea Research*, **30**, 349–649.

MANTYLA A. W. (1987) Standard seawater comparisons updated. *Journal of Physical Oceanography*, **17**, 543–548.

MANTYLA A. W. and J. L. REID (1983) Abyssal characteristics of the World Ocean waters. *Deep-Sea Research*, **30**, 805–833.

MARTIN M., L. D. TALLEY and R. A. DESZOEKE (1987) Physical, Chemical and CTD Data from the Marathon Expedition, *R/V Thomas Washington* 261, 4 May–4 June 1984. Oregon State University, Ref. 87-15, 213 pp.

REED R. K. (1969) Deep water properties and flow in the central North Pacific. *Journal of Marine Research*, **27**, 24–31.

REID, J. L. (1965) *Intermediate waters of the Pacific Ocean*. Johns Hopkins Press, Baltimore, 85 pp.

REID J. L. (1969) Sea-surface temperature, salinity and density of the Pacific Ocean in summer and winter. *Deep-Sea Research*, **16**, (Suppl.), 215–224.

REID J. L. (1982a) On the use of dissolved oxygen concentration as an indicator of winter convection. *Naval Research Review*, **34**, 28–39.

REID J. L. (1982b) On the mid-depth circulation of the World Ocean. In: *Evolution of Physical Oceanography*, MIT Press, Cambridge, 70–111.

REID J. L. and A. W. MANTYLA (1978) On the mid-depth circulation of the North Pacific Ocean. *Journal of Physical Oceanography*, **8**, 946–951.

RODEN G. I. and B. A. TAFT (1985) Effect of the Emperor Seamounts on the mesoscale thermohaline structure during the summer of 1982. *Journal of Geophysical Research*, **90**, 839–855.

ROEMMICH D. (1983) Optimal estimation of hydrographic station data and derived fields. *Journal of Physical Oceanography*, **13**, 1544–1549.

ROEMMICH D. and T. MCCALLISTER (1989) Large-scale circulation of the North Pacific Ocean. *Progress in Oceanography*, **22**, 171–204.

ROEMMICH D., T. MCCALLISTER and J. SWIFT (1991) A trans-Pacific hydrographic section along latitude 24°N; the distribution of properties in the subtropical gyre. *Deep-Sea Research*, **38** (Suppl.), S1–S20.

STOMMEL H. and A. B. ARONS (1960) On the abyssal circulation of the world ocean—I. Stationary planetary flow patterns on a sphere. *Deep-Sea Research*, **6**, 140–154.

STOMMEL H., E. D. STROUP, J. L. REID and B. A. WARREN (1973) Trans-Pacific hydrographic sections at Lats. 43°S and 28°S: the SCORPIO Expedition—I, Preface. *Deep-Sea Research*, **20**, 1–7.

TALLEY L. D (1985) Ventilation of the subtropical North Pacific: the shallow salinity minimum. *Journal of Physical Oceanography*, **15**, 633–649.

TALLEY L. D. (1991) An Okhotsk Sea Water anomaly: implication for sub-thermocline ventilation of the North Pacific. *Deep-Sea Research*, **38** (Suppl.), S171–S190.

TALLEY L. D. and R. A. DESZOEKE (1986) Spatial fluctuations north of the Hawaiian Ridge. *Journal of Physical Oceanography*, **16**, 981–984.

TALLEY L. D. and T. M. JOYCE (submitted) The double silica maximum in the North Pacific. *Journal of Geophysical Research*.

TALLEY L. D., M. MARTIN, P. SALAMEH and Oceanographic Data Facility (1988a) Trans-Pacific section in the subpolar gyre (TPS47); physical, chemical, and CTD data. Scripps Institution of Oceanography, Reference 88-9, 245 pp.

TALLEY L., N. COLLINS and Oceanographic Data Facility (1988b) SAGA II: physical, chemical, and CTD Data, *Akademik Korolev*, 1 May 1987–9 June 1987. SIO Reference 88-10, 137 pp.

WARREN B. A. and W. B. OWENS (1985) Some preliminary results concerning deep northern-boundary currents in the North Pacific. *Progress in Oceanography*, **14**, 537–551.

WARREN B. A. and W. B. OWENS (1988) Deep currents in the central subarctic Pacific Ocean. *Journal of Physical Oceanography*, **18**, 529–551.

WYRTKI K. (1975) Fluctuations of the dynamic topography in the Pacific Ocean. *Journal of Physical Oceanography*, **5**, 450–459.